True multiomic in situ single-cell imaging revealed massive pathological changes in Alzheimer's disease brain

Bin Wang[1], Yijia Sun[1], Renchao Chen[1], Timothy Wiggin[1], Nicolas Fernandez[1], Yuan Cai[1], Yi Sun[1], George Emanuel[1], Jiang He[1]

1. Vizgen, Inc. Cambridge, MA

Introduction

Our understanding of molecular biology and pathology has been greatly facilitated by recent advances in multiple sequencing technologies, coupled with computational analysis, to detect and count proteins and transcripts. However, these tools lack spatial resolution and are unable to map gene expression and cell-cell interaction in a tissue context. Due to the complexity of tissue biology, integrated codetection of proteins and mRNAs from the same cell has the potential to not only reveal the correlation between these two classes of biologically important molecules, but also help understand the mechanisms of gene regulation, at both the transcriptional and translational levels.

Alzheimer's disease (AD) is currently ranked as the seventh leading cause of death in the United States and is the most common cause of dementia among older adults. Advancements in research have proved fruitful with the recent FDA approved drug Aducanumab (Aduhelm™) from Biogen but further work is needed to drive more effective treatments. The two disease hallmarks: abnormal protein aggregates β-Amyloid plaque (Aβ) and hyperphosphorylated tau Neurofibrillary tangles (NFTs), together with other misfolded proteins during disease progression, cannot be revealed by RNA transcript detection. To address the need for multiomic measurements, Vizgen has recently launched protein codetection products and developed a protocol that allows detection of selected protein targets mapped together with a spatially resolved transcriptomic profile on the MERSCOPE™ Platform.. With downstream multiomic data analysis and MERSCOPE™ Vizualizer software, Aβ/tau proteins and selected gene panel are mapped with respective expression profile to the whole brain section with high resolution. The new MERSCOPE™ protein codetection workflow enables true multiomic analysis and leveraging this comprehensive biological information can drive AD research to ultimately find a cure.

Materials & Methods

MERFISH is a massively multiplexed single-molecule imaging technology for spatially resolved transcriptomics capable of simultaneously measuring the copy number and spatial distribution of hundreds to tens of thousands of RNA species across a whole tissue slice (Fig. 1).

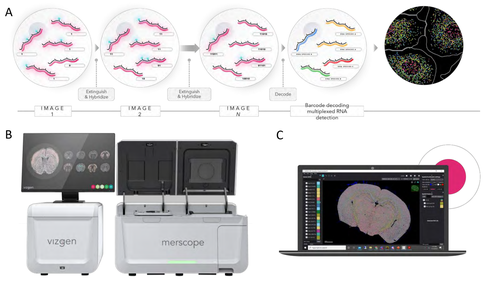

Figure 1. A, Illustration of MERSCOPE™ workflow. To perform MERFISH, target RNA species are labeled with a tile of oligo probes containing different barcodes. Each barcode is then fluorescently detected in sequential round of imaging, and the optical barcode generated from these multiple rounds of imaging with '1' indicating fluorescence signal and '0' indicating no fluorescence, will help to resolve different RNA species. B, Vizgen's commercially available MERSCOPE Platform. C, data visualization by MERSCOPE Vizualizer software.

To enable RNA-protein codetection capabilities, we designed oligonucleotide conjugated secondary antibodies, targeting host species of Mouse, Rabbit, Goat, Rat, Human, and Chicken, via indirect immunofluorescence (IF) staining (Fig. 2A-B). The protein codetection workflow involves three protocols the first enables verification of antibody performance in regular IF, the second allows verification of antibody performance and detection by the MERSCOPE™, and the third allows protein codetection with MERFISH. Primary antibodies targeting proteins of interest were first verified to work within IF using a standard IF protocol. Upon successful regular IF staining, the primary antibodies were then further verified using the MERSCOPE™ Protein Stain Verification kits and MERSCOPE™ Protein Stain kits using a short verification workflow (~ 1h) on the MERSCOPE platform. Once verified, we proceeded with a full MERSCOPE run with protein codetection (Fig. 2C).

Figure 2. A, illustration of the design of protein codetection antibodies. B, MERSCOPE protein stain reagents products. C, MERSCOPE RNA-Protein codetection workflow.

Results

MERSCOPE workflow resulted in highly accurate and sensitive in- situ single-cell transcriptomic imaging

In order to establish MERFISH protein codetection and investigate molecular changes at both protein and transcripts level in Alzheimer's disease, we selected three disease-related protein targets: mouse monoclonal anti-pTau clone AT8 (recognizes tau protein phosphorylated at both serine 202 and threonine 205), rabbit monoclonal anti-Aβ clone mOC23 [recognizes an aggregation-dependent epitope of Aβ that maps to a linear segment of Aβ (residues 2-6, AEFRH)], rat monoclonal anti-TDP-43 (target nonphosphorylated peptide corresponding to the C-terminal domain of human TDP43, which includes serine residues 409 and 410), together with three cell-type specific and structural protein targets: goat anti-smooth muscle actin (SMA), human anti-Myelin Basic Protein (MBP, oligodendrocytes) and chicken anti-Glial Fibrillary Acidic Protein (GFAP, glial astrocyte). We used a gene panel of 244 genes for MERSCOPE together with these antibodies using two aged brain samples (from two human patients) and two AD brain samples (two brain regions from the same AD patient) (Fig. 3A). For the MERSCOPE results, >50 million transcripts were detected from the two aged brain samples and >17 million transcripts were detected in the two AD brain samples. There were over 27,000 transcript counts per FOV in the two aged brains and about 6,000 transcript counts per FOV in two AD brain samples (Fig. 3B-C). The two aged brains displayed a high correlation (r=0.98) while the two AD brain samples also displayed a high correlation (r=0.99) as well (Fig. 3D-E). We next compared MERSCOPE results to bulk sequencing (normal brain-cortex) and found strong correlations in the two aged brain samples (r=0.76 and r=0.75 respectively), and slightly lower correlations in the two AD brain samples (r=0.65 and r=0.68 respectively) which implied the existence of significant molecular/ neuropathological changes in AD brains (Fig. 3F-I).

A

Brain Sample Name	Sample ID	Gender	Age	Tissue Type	Clinical Diagnosis	RIN	DV200
Aged brain #1	1156141F	Male	77	Normal region	n/a	6.4	62.89
Aged brain #2	22676A1	Male	80+	Normal region	Alzheimer's disease	6.6	71.27
AD Patient brain Block #1	1165882F	Female	67	Diseased region	Alzheimer's disease	5.1	60.75
AD Patient brain Block #2	1165882F	Female	67	Diseased region	Alzheimer's disease	5.4	60.00

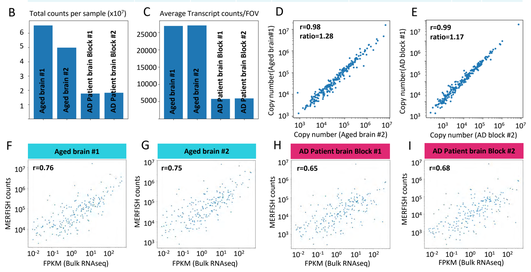

Figure 3. Protein codetection MERFISH on aged brains and AD patient brain blocks. B, total transcript counts per sample. C, average transcript counts per FOV per experiment. D-E, gene expression correlation between two aged brains (D) and two AD patient brain blocks (E). F-I, correlation coefficiency between each experiment and bulk RNAseq data (**normal brain-cortex**).

True multiomic imaging from protein codetection on MERSCOPE

To visualize the successful MERFISH protein codetection, we used the MERSCOPE Vizualizer to display spatial distribution of transcripts from 244 genes and the six selected protein targets. More RNA transcripts were detected in two aged brain samples (Fig. 4A-B) than in two AD brain blocks (Fig. 4C-D). Six protein targets were also successfully stained with high resolution and visualized (Fig. 4, bottom row showing costain of five targets). To our surprise, we detected AD hallmarks (Aβ/p-Tau) in some regions of aged brain #2, although it was a normal brain region based on sample information. This discovery highlighted the advantage of MERFISH protein codetection as these pathological hallmarks could not be unveiled by RNA transcripts.

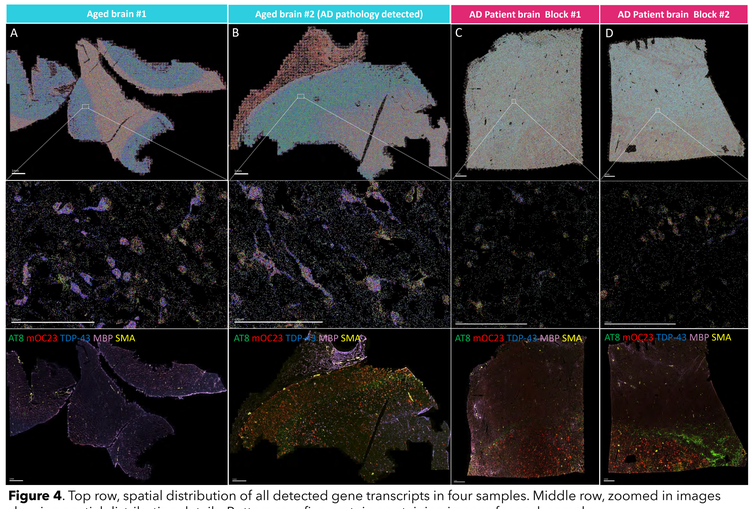

Figure 4. Top row, spatial distribution of all detected gene transcripts in four samples. Middle row, zoomed in images showing spatial distribution details. Bottom row, five protein co-staining images for each sample.

High resolution six-plex protein codetection on MERSCOPE

Because protein codetection on MERSCOPE was performed with high resolution, we next focused in the grey matter cortical regions and examined the molecular changes between normal aged brain and AD brain samples. In aged brain #1, all the disease-related protein targets (AT8, mOC23, and TDP-43) were undetected indicating while other cell-type specific and structural proteins (SMA, GFAP, and MBP) were detected in high sensitivity. DAPI and PolyT images highlighted all cells in the region and were used in cell segmentation (Fig. 5).

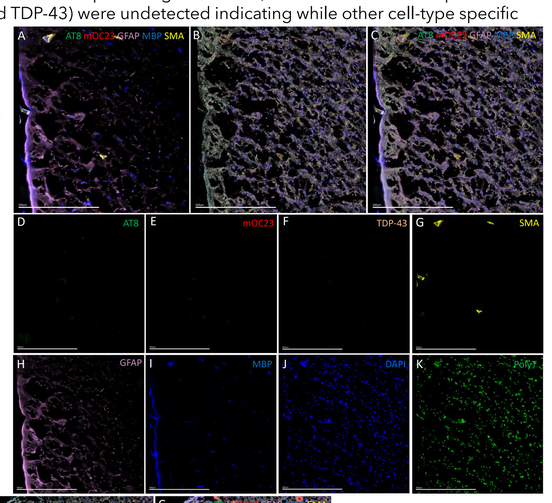

Figure 5. Representative images of protein codetection MERFISH on normal aged brain #1. A, five protein co-staining image in a small grey matter region. B, spatial distribution of all 244-gene transcripts. C, overlapped image of A and B containing spatial information of both protein targets and RNA transcripts (including copy number). D-I, individual protein stain. J, DAPI staining. K, PolyT staining showing all mRNA transcripts.

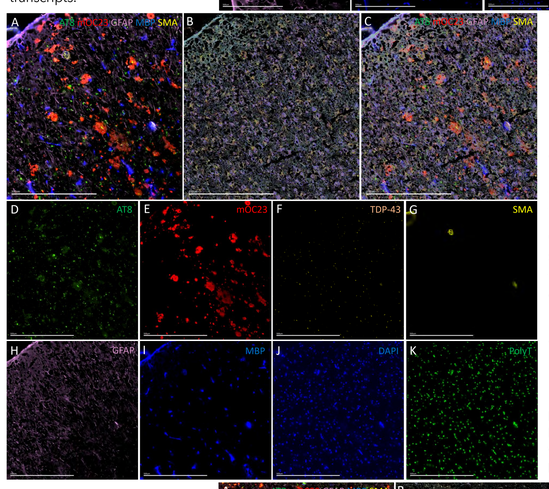

However, in aged brain #2, we detected significant amounts of pathological proteins, including amyloid plaques (by mOC23) and hyperphosphoryloated tau (by AT8). Moreover, TDP-43 nuclei signal was detected in grey matter spatially close to Aβ and tau deposits indicating widespread TDP-43 pathology within the aged brain #2 (Fig 6).

Figure 6. Protein codetection MERFISH on aged brain #2 with AD and TDP-43 pathology.

In the AD brain block #2, we detected massive amyloid plaques (by mOC23) and hyperphosphoryloated tau (by AT8) with no TDP-43 signal, indicating that this sample is from an AD patient with no TDP-43 pathology. As expected, SMA, GFAP and MBP proteins were also successfully codetected(Fig. 7). AD brain block #1 displayed similar staining.

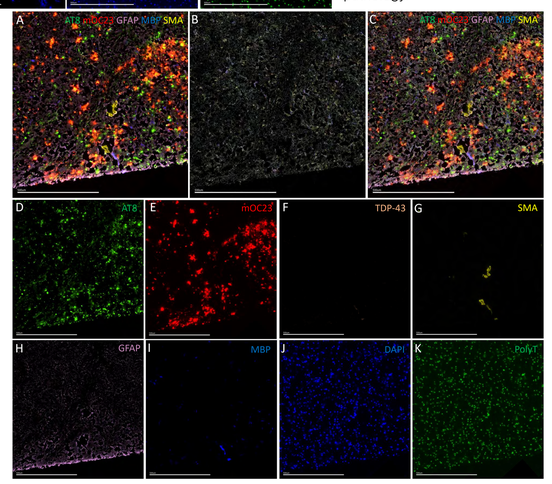

Figure 7. Protein codetection MERFISH on AD patient brain block #2.

Pathological changes revealed by protein codetection MERFISH by MERSCOPE

We next examined and compared a few selected genes and proteins between normal aged brain #1 and aged brain #2 (AD pathology detected) in cerebral cortex subregion. MBP and GFAP proteins were both found increased in aged brain #2 (AD pathology detected) using antibody staining indicating an elevated neuroinflammation level. This matched the *gfap* transcript increase detected in this brain region. Another example, *aqp1* (Endothelial Aquaporin-1) gene also increased in aged AD brain . In the contrast, transcripts from genes *glul* and *snap25* were both at lower levels accompanied by large increase of Aβ deposits and tau hyperphosphorylation seen by protein co-staining. indicating reduced neuronal transmission activity and gradual loss of synaptic function in aged AD brain (Fig. 8).

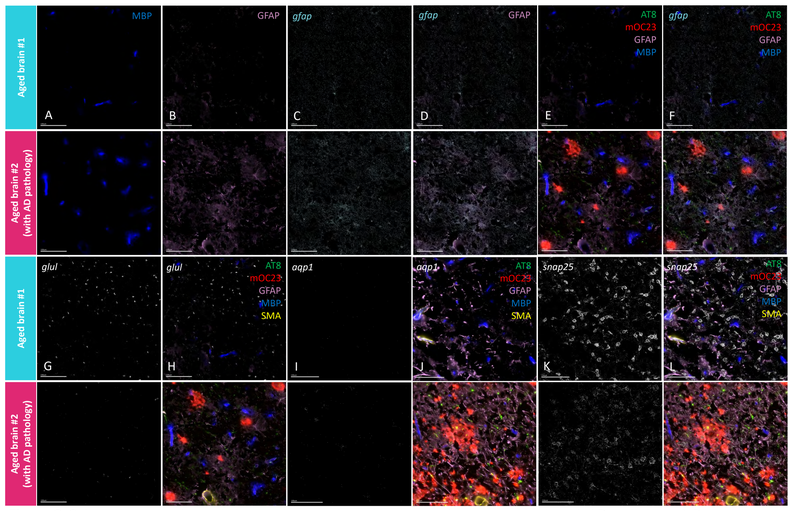

Figure 8. Selected gene and protein images in normal aged brain sample and aged brain with AD pathology. A-B, protein staining images of MBP and GFAP. C, distribution of gene *gfap*. D, both gene *gfap* and protein GFAP. E, four selected protein images. F, gene *gfap* and four selected protein images. G-H, gene *glul* and overlapping with five protein co-staining images. I-J, gene *aqp1* and overlapping with five protein co-staining images. K-L, gene *snap25* and overlapping with five protein co-staining images.

Single cell, spatially resolved transcriptomic profiling on human brain

Lastly, we performed signal-cell analysis on the MERFISH protein codetection data using one normal aged brain and one AD brain as examples. With high spatial resolution, MERSCOPE enabled characterization of gene expression at single-cell level and helped to identify 16 cell clusters in normal aged brain #1 and 12 cell clusters in AD patient brain block #2 with UMAP, based on transcriptome similarity (Fig. 9 and Fig. 10).

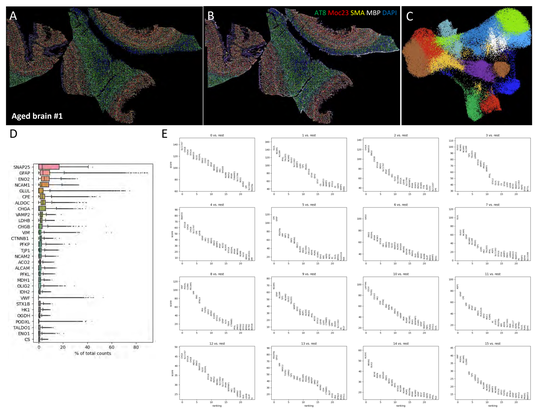

Figure 9. Single-cell clustering analysis. A, spatial distribution of sixteen identified cell types in normal aged brain #1. B, overlapped sixteen cell clusters with four protein staining images as well as DAPI, C, UMAP. D, Top expressing gene list. E, Top expressing genes in each identified cell cluster versus other clusters.

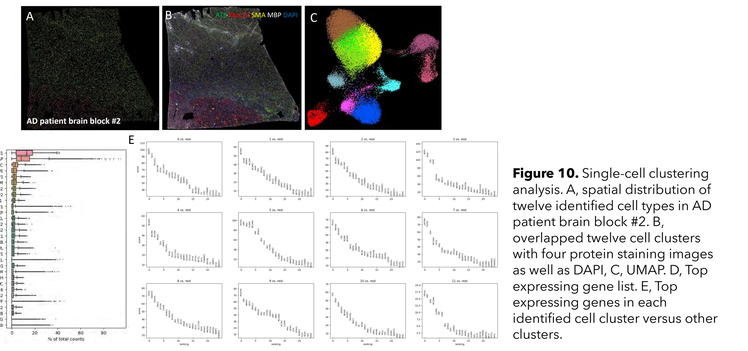

Figure 10. Single-cell clustering analysis. A, spatial distribution of twelve identified cell types in AD patient brain block #2. B, overlapped twelve cell clusters with four protein staining images as well as DAPI, C, UMAP. D, Top expressing gene list. E, Top expressing genes in each identified cell cluster versus other clusters.

Conclusion

1) We successfully used the MERSCOPE Protein Stain Kits to generate both gene expression and protein detection in situ with spatial context within human brain samples
2) We detected and visualized widespread presence of AD hallmark proteins from a normal region of an AD patient.
3) MERSCOPE protein codetection revealed massive pathological changes (both protein and RNA) in AD brain, as compared to normal aging brain.
4) MERSCOPE protein codetection can provide additional biological information in relevant to gene transcripts as revealed by spatial localization when viewing protein and RNA transcripts simultaneously.

In summary, the streamlined MERSCOPE protein stain kits enables us to gain both gene expression and protein abundance in situ within spatial context. This will provide critical insights for understanding the cellular functions in physiological and pathological processes within the brain.